Hindawi
The Scientific World Journal
Volume 2020, Article ID 2187129, 8 pages
https://doi.org/10.1155/2020/2187129

Research Article

Valorization of Oued Sebou Natural Sediments (Fez-Morocco Area) as Adsorbent of Methylene Blue Dye: Kinetic and Thermodynamic Study

Abdelaziz Dra,[1] Karim Tanji,[1] Abdellah Arrahli,[1] El Mustafa Iboustaten,[1] Abdelali El Gaidoumi,[1,2] Achaimae Kherchafi,[1] Aziz Chaouni Benabdallah,[1] and Abdelhak Kherbeche[1]

[1]*Laboratory of Catalysis, Materials and Environment, Higher School of Technology, Sidi Mohamed Ben Abdellah University of Fez, 30000 Fez, Morocco*
[2]*Higher School of Technology of Khenifra, Sultan Moulay Slimane University, Beni Mellal, Morocco*

Correspondence should be addressed to Karim Tanji; karimtanji1992@gmail.com

Received 9 November 2019; Revised 15 February 2020; Accepted 6 March 2020; Published 19 May 2020

Academic Editor: Ghadir A. El-Chaghaby

The objective of this study is to evaluate the efficiency of methylene blue removal using Oued Sebou sediments as an adsorbent. The presence of carboxyl functional group demonstrated by infrared (IR) analysis of the sediment favorized the methylene blue (MB) adsorption. Sediment collected from Oued Sebou could remove the most MB molecules at pH 8. The Freundlich model described suitably the adsorption process. The experimental measured enthalpy (ΔH) and entropy (ΔS°) are 118.1 kJ mol^{-1} and 395.2 J mol^{-1} K^{-1}, respectively, indicating that the reaction was endothermic with an increase of randomness at the solid/liquid interface during the adsorption. The kinetics of MB adsorption by sediment were adequately fitted to the pseudo-second-order model. Experimental results showed that the adsorption capacity of the methylene blue dye depends on the solution pH, the initial dye concentration, the adsorbent mass, the sediment particle diameter, and the temperature of the reaction medium. The removal efficiency of the MB molecules reaches 100% after 60 minutes under the optimum conditions.

1. Introduction

Many industries such as textiles and printing are continuously releasing various pollutants into the hydrosphere, and these pollutants have adverse impacts on the environment and human health [1]. They can cause eye burns, which result in permanent damage to human and animal's eyes, its inhalation may give rise to breathing difficulties, and its ingestion through the mouth causes a burning sensation, nausea, vomiting, sweating, and an abundance of cold sweats [2]. Many research works have studied the removal of dyes from aqueous solution [3, 4], and the adsorption property of several natural adsorbents was widely studied [4–7]. Nevertheless, according to the bibliography, little effort has been made to study the adsorption of MB by using sediments as an adsorbent. The color produced by minute amounts of organic dyes in water is of a great concern because the color in water is aesthetically unpleasant. As such, few dyes and their degraded forms are carcinogenic and toxic [8]. Methylene blue is one of the most commonly used dyes for dyeing cotton, wool, silk, and leather. The dye is not toxic in nature, and it causes several harmful effects to the health of living beings, though. Once consumed, methylene blue can cause increased heartbeat, nausea, and vomiting. Today, several physical or chemical processes are used to treat dye laden wastewaters such as photodegradation [9]. The sediments are often called "vases", and we define the constitution as a more or less large set of particles or precipitates which have undergone transport in their individual parts [10].

The current work aims at investigating the adsorption capacity of Oued Sebou sediments on the elimination of methylene blue. The effect of operational parameters such as

adsorbent loading, initial dye concentration, particles size, and pH was studied. Besides, the modeling of the adsorption kinetics and thermodynamics was studied as well. The adsorption isotherm models were investigated to explain the adsorption mechanism at the equilibrium during the elimination of MB from aqueous solutions.

2. Materials and Methods

2.1. Materials. The sediment adsorbent is obtained from Moroccan Oued Sebou. The sediment samples were taken with a shovel at the top of the fine sediment deposit in a layer between 5 and 15 cm of the depth. Next, it was dried, grinded, and sieved before adsorption applications. Selected concentrations of MB solutions (10–50 mg L^{-1}) were prepared in distilled water at room temperature. During the adsorption experiment, HCl (0.5 M) and NaOH (0.5 M) were used to regulate the solution pH.

2.2. Characterization Techniques. The X-ray diffraction (X′ PERT PRO), infrared spectroscopy (VERTEX 70), and SEM-EDAX (QUANTA 200) were used to identify the composition and the morphology of the sediment material. During adsorption tests, the remaining concentration of MB was determined by measuring the absorbance at 66 2 nm using a spectrophotometry UV-visible (VR-2000).

2.3. Adsorption Experiment. The adsorption experiments of MB by the sediment were carried out by using a mass of adsorbent mixed with a solution of MB at room temperature under continuous stirring. In order to investigate the kinetic adsorption, a 5 mL of the sample was collected every 5 min to measure its concentration by spectrophotometric UV-vis, but, before that, the suspension was filtered with a filter paper with 0.45 μm pore size to separate the sediment particles from the liquid.

The removal of MB molecules was calculated using following formula [11, 12]:

$$\text{removal } (\%) = \frac{(C_0 - C_t)}{C_0} \times 100, \quad (1)$$

where C_0 and C_t are the concentrations of MB at $t = 0$ and at $t \neq 0$, respectively.

The adsorption capacity of the sediment for MB removal was obtained applying the following equation [13]:

$$q_e = \frac{(C_0 - C_e)}{m} \times V, \quad (2)$$

where q_e (mg. g^{-1}) is the adsorption capacity at equilibrium; C_0 (mg. L^{-1}) is the initial concentration of MB; C_e (mg. L^{-1}) is the equilibrium concentration of MB; V (L) is the MB solution volume; and m (g) is the sediment mass.

The influence of operating conditions on the adsorption of MB onto the sediment was studied in a batch system by varying the sediment mass from 1 to 2 g L^{-1}, the initial MB concentration from 10 to 50 mg·$L^{-1,}$ and the pH solution in the range of 4–10.

3. Results and Discussion

3.1. Sediment Characterization

3.1.1. X-Ray Diffraction (XRD). The mineralogical characterization of sediments is presented in Figure 1. The obtained diffractogram showed different crystalline phases: muscovite ($KAl_3Si_3O_{10}(OH)_2$), anhydrite ($CaSO_4$), calcite ($CaCO_3$), hematite (Fe_2O_3), halite (NaCl), quartz (SiO_2), and dolomite (CaMg $(CO_3)_2$) [11, 14, 15].

3.2. Fourier Transform Infrared Spectroscopy. Infrared analysis was used to identify all absorption bands corresponding to the different vibrations of the characteristic bonds of the phases detected by XRD. Figure 2 shows that bands at 776 and 870 cm^{-1} corresponding to the vibration stretching of Si-O-Al and CO_3^{2-}, respectively, while the band at 946 cm^{-1} is attributed to the vibrations of the quartz Si-O-Si bonds. The H-O-H bonds are characterized by an intense band at 3425 cm^{-1} and 1421 cm^{-1} corresponding to the valence vibrations of the Si-O-Si bond [16].

3.3. Scanning Electron Microscopy (SEM-EDX). Scanning electron microscopy (SEM) was used to observe the morphology and the particles size of the sediment. Figure 3 illustrates the corresponding images. It was demonstrated that there are grains of different morphologic materials. The quantitative chemical analysis is performed by EDX. Figure 4 shows the existence of a proportion of iron, aluminum, calcium, and magnesium in the sediments, which is related to the presence of hematite, calcium carbonate, and dolomite phases [17].

4. Adsorption Study

4.1. Effect of the Particle Size. In order to study the effect of sediment particles sizes, a series of experiments were performed with a constant adsorbent mass of 1g·L^{-1}, initial dye concentration of 40 mg·L^{-1}, initial pH, and different sizes of sediment particles thanks to grinding and sieving with sieves of different diameter (40, 63, 125, and 200 μm). Figure 5 illustrates that decreasing particle size enhanced the adsorption capacity: the 40 μm particle size has the highest methylene blue removal rate (95%). Other treatments showed lower removal rate between 72% and 85.6%, although the 200 μm processing showed slow adsorption about 51.64% at 60 min. This evolution could be explained by the link between the effective surface area of sediment particles and adsorption efficiency [18].

4.2. Effect of pH. The study of the effect of pH on the adsorption of MB using the sediment shows the affectation of its surface properties, particularly its functional groups, which influences the overall adsorption process. The effect of the MB solution pH on the adsorption experiment using 1g·$L^{-1}$of Oued Sebou sediments and 40 mg·L^{-1} as MB concentration at room temperature was studied. The pH

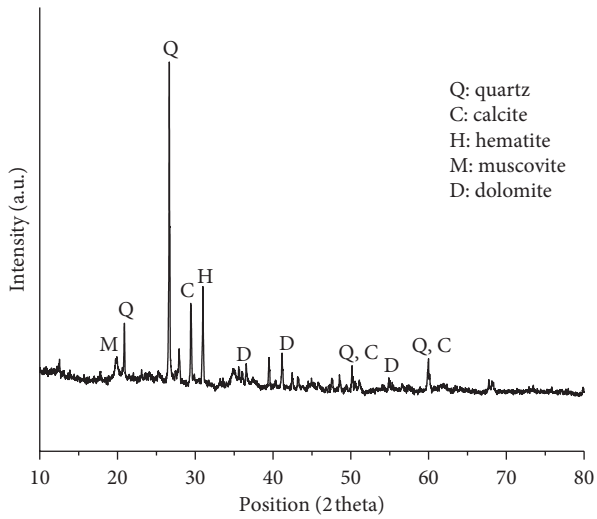

Figure 1: X-ray diffraction of Oued Sebou sediment.

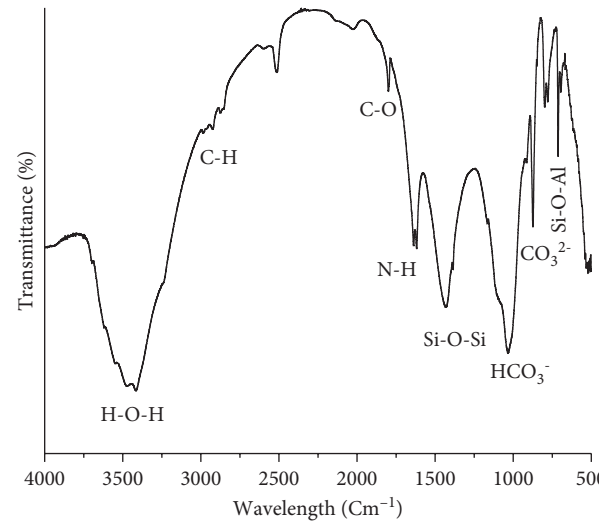

Figure 2: Infrared spectrum of Oued Sebou sediment.

range of the solution has been adjusted from 4 to 10 using HCl (0.5 M) and NaOH (0.5 M). It has been observed that MB removal increases by rising the dye solution pH [19] where it reaches its maximum at pH 8 and 10 (Figure 6). This behavior can be explained by the case of basic dyes (MB) at acidic pH, and H^+ ions will compete with blue methylene cations, which will reduce adsorption efficiency. On the other hand, when the pH is considered, the basic of this competition decreases when the active sites become more negatively charged on the sediment surface, which enhances the MB adsorption by electrostatic attraction forces [20]. As a result, we can conclude that the surface sediment is negatively charged. For further MB adsorption tests, pH 8 was fixed as the optimum solution pH .

4.3. Effect of Initial Dye Concentration. For evaluating the adsorption capacity of sediments according to initial dye concentration, this parameter was varied in a range of 10–50 $mg{\cdot}L^{-1}$. Figure 7 illustrates the evolution MB adsorption by sediments for different initial MB concentrations. The results revealed that the adsorption removal efficiency of MB decreases from 98% to 78% with the decrease of the initial MB concentration from 50 to 10 $mg{\cdot}L^{-1}$. This rate evolution could be explained by the low dispersion of MB molecules into sediments due to the high MB concentration. Furthermore, the high MB concentration saturates the sediments, which decreases the adsorption capacity [21].

4.4. Effect of Adsorbent Mass. The results of sediment mass effect on the MB adsorption are shown in Figure 8. The results indicate that the removal efficiency of MB adsorption onto the Oued Sebou sediment increased from 79% to 94% when the sediment mass increased from 1 to 2.5 $g\,L^{-1}$. These observations are in accordance with the increase of active sites on the sediment surface [22]. Nevertheless, the dye removal remains constant while the sediment dose is up to 2 $g\,L^{-1}$. Therefore, the optimal sediment dose for maximal MB elimination was fixed at 2 $g\,L^{-1}$.

4.5. Effects of Temperature and Activation Energy. Although the effect of temperature on adsorption has been carefully studied, no universal law has been found. Indeed, these studies have shown that an increase in temperature can lead to either an increase or a decrease in the amount of molecules adsorbed [23, 24]. To study the effect of temperature on the kinetics of MB adsorption by the sediment, the experiments were carried out in a temperature ranging from 283 K to 323 K. The results obtained are shown in Figure 9, which indicate that there is a higher temperature, and the sediment produces higher removal efficiency of MB. According to this result, enough energy ameliorates the adsorption fixation of MB [21].

4.6. Kinetic Models. In order to investigate the kinetic model of methylene blue adsorption, the following equations were used [25]:

$$\ln\left(q_e - q_t\right) = \ln\, q_e - k_1 t \;\text{pseudo} - \text{first} - \text{order}\,(\text{PFO}),$$

$$\frac{t}{q} = \frac{1}{k_2 q_e^2} + \frac{t}{q} \;\text{pseudo second} - \text{order}\,(\text{PSO}). \tag{3}$$

where q_e is the adsorption capacity at equilibrium, q_t is the adsorption capacity at different time, k is the kinetic constant, and t is the time.

It is concluded from Table 1 that the values of the pseudo-first-order (PFO) R^2 were 0.967, 0.991, 0.998, 0.75, and 0.947; the values of the pseudo-second-order (PSO) R^2 were 0.997, 0.994, 0.986, 0.996, and 0.991; thus, R^2 of the PSO was bigger than that of the PFO, implying that the pseudo-second-order kinetic was the main kinetic process as long as it gives the best prediction for the kinetic data [26]. Similar results were observed by Lamia Dali et al. using an Algerian

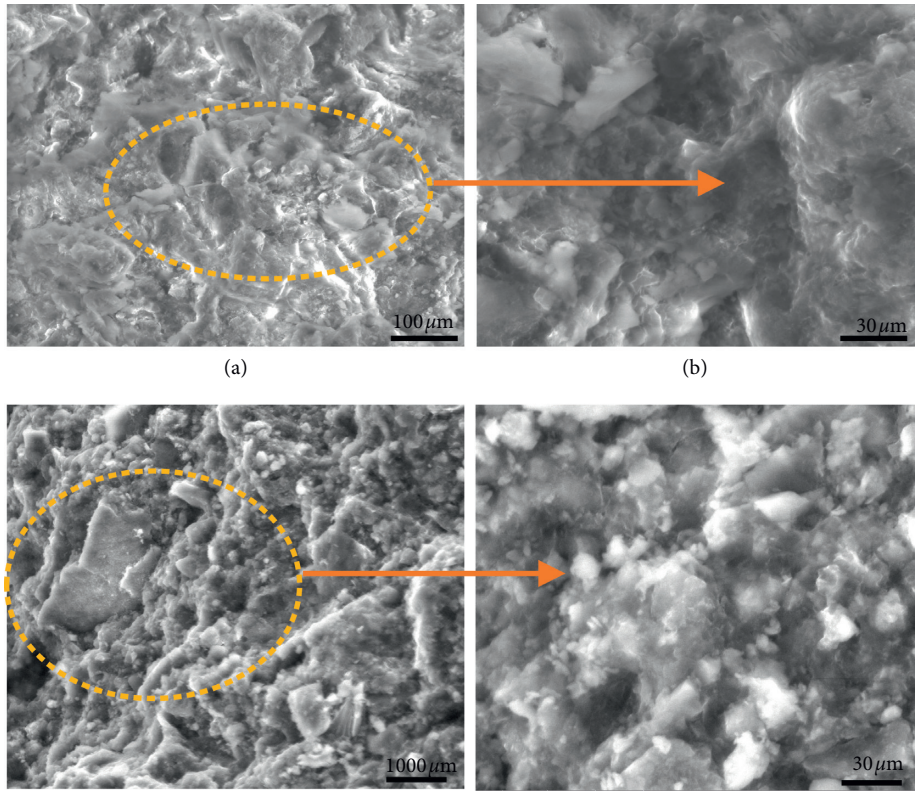

Figure 3: SEM images of Oued Sebou sediment.

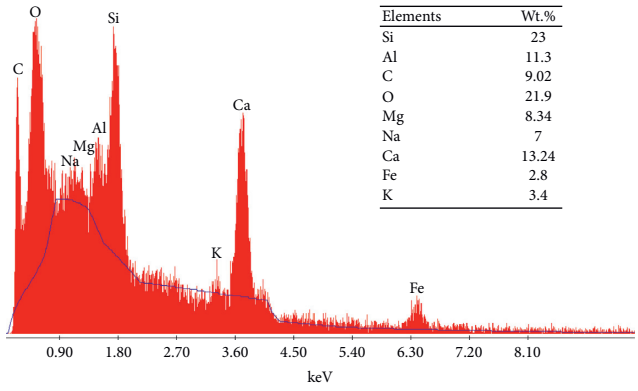

Elements	Wt.%
Si	23
Al	11.3
C	9.02
O	21.9
Mg	8.34
Na	7
Ca	13.24
Fe	2.8
K	3.4

Figure 4: EDX microanalysis spectrum of Oued Sebou sediment.

palygorskite [21], Therefore, adsorption is an irreversible reaction, and it implies both the rapid fixation of the dye molecules and long fixation on the weak energy sites [27].

4.7. Isotherm Models. Isotherm models (Langmuir, Freundlich, and Dubinin–Radushkevich) were studied to explain the adsorption system at equilibrium [28]. All isotherms are executed with a variation of MB concentration from 10 to 50 mg·L^{-1}. The results of adsorption isotherms show that the adsorption process of MB onto sediment adsorbate fitted more strictly the Freundlich isotherm equation

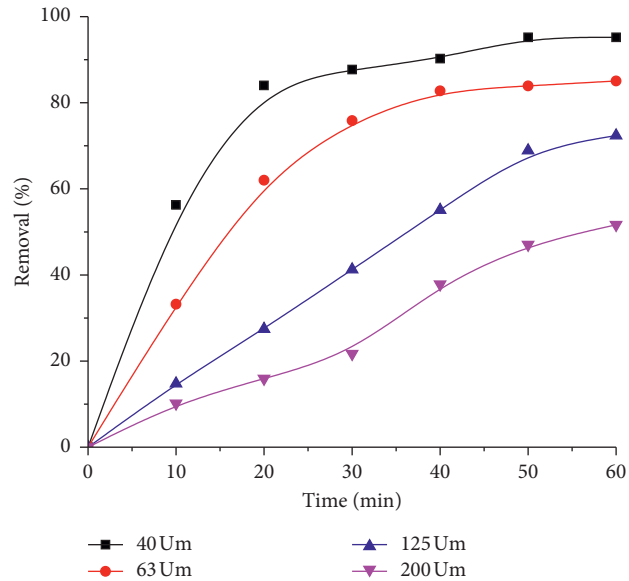

Figure 5: MB removal at different particle sizes.

(equation (5)) than the Langmuir (equation (4)) and Dubinin–Radushkevich (equation (6)) isotherms [29]. This result is based on the higher value of R^2 (0.998), which is considered as a measure of the excellent fit of experimental data on the isotherms models. Thus, this process is a nonideal sorption on heterogeneous surfaces and multilayer sorption [30].

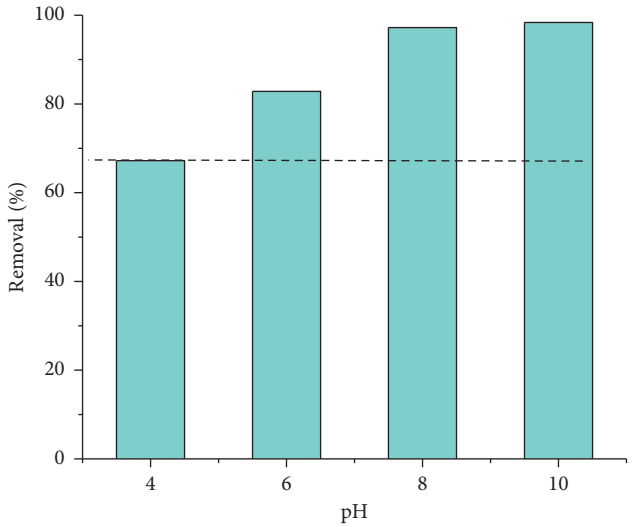

Figure 6: Effect of pH on MB removal.

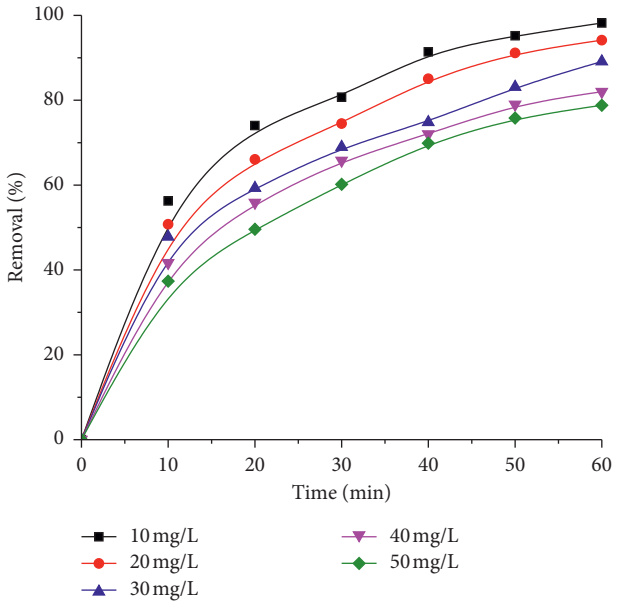

Figure 7: Effect of initial MB concentration.

The Langmuir isotherm admits that adsorptions happen at specific homogeneous active sites on the adsorbent surface. Its corresponding equation is explained as follows:

$$\frac{C_e}{q_e} = \frac{C_e}{q_m} + \frac{1}{K_L.q_m}, \quad (4)$$

where K_L is the Langmuir constant ($L{\cdot}mg^{-1}$).

The Freundlich model describes nonuniform and multilayer adsorption on heterogeneous surfaces. Its equation model is detailed as follows:

$$\log q_e = \log K_F + \frac{1}{n}\log C_e, \quad (5)$$

where K_F the adsorption capacity and $1/n$ the intensity of adsorption.

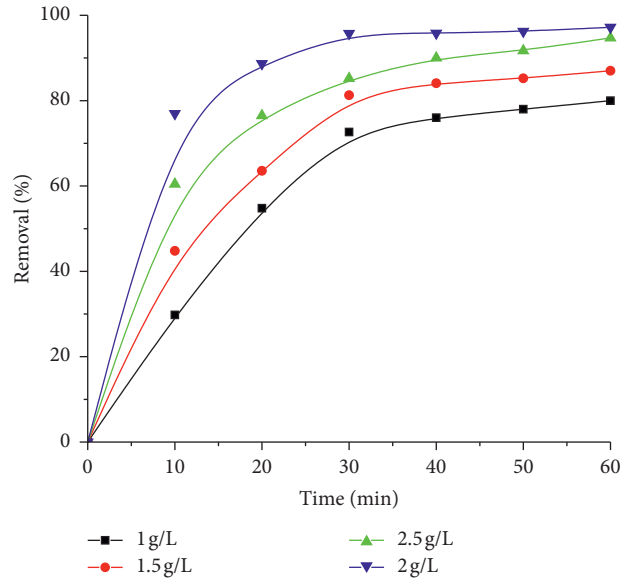

Figure 8: Effect of adsorbent mass.

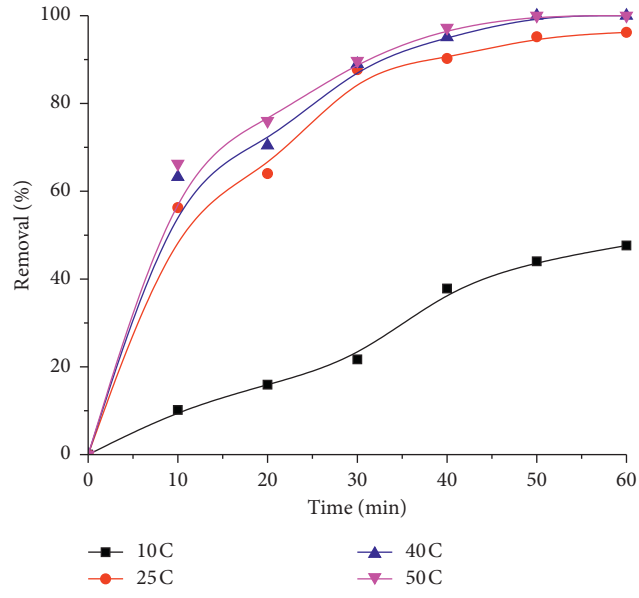

Figure 9: Temperature effect on MB removal.

The Dubinin–Radushkevich (D–R) model is used to determine the nature of adsorption [25, 27, 28]. The equation form of the D–R isotherm is as follows:

$$\ln q_e = \ln q_{mDR} - K_{DR}\varepsilon^2, \quad (6)$$

where q_{mDR} is the sediment adsorption capacity at equilibrium ($mg{\cdot}g^{-1}$), K_{DR} is the Dubinin–Radushkevich constant ($mol^2{\cdot}kJ^{-2}$), and ε is the Polanyi potential ($J{\cdot}mol^{-1}$).

The corresponding data of the three models are presented in Table 2.

4.8. Adsorption Thermodynamic Studies. The Van't Hoff equations were used to determine the thermodynamic parameters, mainly Gibbs free energy change (ΔG°), enthalpy

Table 1: Pseudo-first-order and pseudo-second-order parameters for adsorption of methylene blue ions onto sediments at different concentrations.

		Pseudo-first-order			Pseudo-second-order		
MB concentration ($mg{\cdot}L^{-1}$)	q_e, experimental ($mg{\cdot}g^{-1}$)	k_1 (min^{-1})	q_e, calculated ($mg{\cdot}g^{-1}$)	R^2	k_2 ($g{\cdot}mg^{-1}$ min^{-1})	q_e calculated ($mg{\cdot}g^{-1}$)	R^2
10	4.90	$2.7.10^{-3}$	3.78	0.967	5.10^{-4}	5.84	0.997
20	9.41	$9.2.10^{-3}$	3.25	0.991	$6.9.10^{-4}$	11.07	0.994
30	13.37	$2.9.10^{-2}$	2.13	0.998	$2.2.10^{-4}$	16.39	0.986
40	16.40	$4.9.10^{-2}$	1.39	0.75	$1.1.10^{-4}$	20.38	0.996
50	19.70	$6.4.10^{-2}$	4.01	0.947	5.10^{-5}	26.45	0.991

Table 2: Adsorption isotherm constants for MB adsorption onto the sediment.

Langmuir isotherm parameters			Freundlich isotherm parameters			Dubinin–Radushkevich isotherm parameters			
q_m	K_L	R^2	n	K_F	R^2	q_m	K_{DR}	E	R^2
3.24	5.268	0.953	0.395	0.004	0.998	3.332	0.030	4.082	0.950

Table 3: Thermodynamic parameters of MB adsorption onto the sediment.

ΔG° ($kJ{\cdot}mol^{-1}$)				ΔH° ($kJ{\cdot}mol^{-1}$)	ΔS° ($J{\cdot}mol^{-1}.\ K^{-1}$)
$T = 283$ K	$T = 298$ K	$T = 313$ K	$T = 323$ K		
0.39	5.52	9.47	13.42	118.1	395.2

change (ΔH°), and entropy change (ΔS°), of the adsorption process from the experimental data and the following equations:

$$\Delta G^\circ = -\mathrm{RT}\cdot\mathrm{LnKL},$$

$$\mathrm{LnKL} = \left(\frac{\Delta S^\circ}{R}\right) - \left(\frac{\Delta H^\circ}{\mathrm{RT}}\right), \quad (7)$$

$$\Delta G^\circ = \Delta H^\circ - T\cdot\Delta S,$$

where ΔG° is the standard free energy, $kJ\,mol^{-1}$; T is the absolute solution temperature, K; ΔH° is the standard enthalpy, $kJ\,mol^{-1}$; R is the universal gas constant, $8.314\,J\,mol^{-1}\,K^{-1}$; and ΔS° is the standard entropy, $J\,K^{-1}$.

The linear plots of ln K_L versus 1/T afford ΔH and ΔS values for the adsorption of methylene blue at different temperatures. The enthalpy values imply that the adsorption is endothermic [31, 32].

The value of ΔS° is positive, which means the increase of randomness at the solid/liquid interface during the adsorption process, as reported by Aroğuz et al. in their work on MB removal by the pyrolyzed petrified sediment [25]. Contrariwise, Gülen et al. found that the enthalpy, entropy, and Gibbs values are negative during the removal of methylene blue by using an porous carbon adsorbent [33], which confirms that the adsorbent type controls the thermodynamic parameters over the adsorption process.

Table 3Values of studied thermodynamic parameters.

4.9. Comparison of the Adsorption Efficiency with Literature Studies. The efficiency of the adsorption removal and the contact time on methylene blue, according to the literature, is presented in Table 4 compared to our work. As it can be noticed in Table 4, the different materials used for the adsorption of the MB dye compared with the adsorption of MB by the sediment shows an important effective removal yield with a fast contact time.

Table 4: Comparison of the adsorption efficiency of methylene blue on various literature studies.

Adsorbent	Adsorption removal (%)	Reference
CFS clay	95% (24 h)	[34]
Polyamide-vermiculite	35% (120 min)	[35]
Algerian palygorskite	100% (20 min)	[36]
Montmorillonite clay	100% (35 min)	[37]
Moroccan cactus	63% (60 min)	[37]
Moroccan sediment	100% (60 min)	Present work

5. Conclusion

During this work, batch studies on adsorption of methylene blue molecules using a Moroccan sediment of Oued Sebou without any further treatment obviously suggest that the maximum adsorption yield was found as 100% at pH equal to 8, 323 K as the solution temperature, $1g{\cdot}L^{-1}$ of mass sediment, and $10\,mg{\cdot}L^{-1}$ as MB concentration, which proves that those operational parameters greatly affected the adsorption process. Throughout limited conditions, the adsorption behaves well at low concentration and becomes more efficient at increasing sediment masses. The highest adsorption removal is obtained at basic pH at higher temperatures. The pseudo-second-order and Freundlich isotherm models are well fitted with the adsorption process. This experimental result showed that the adsorption removal

of the methylene blue dye is interesting using a friendly natural material from Morocco.

Data Availability

No data were used to support this study.

Conflicts of Interest

The authors declare that they have no conflicts of interest.

References

[1] L.-F. Chen, H.-H. Wang, K.-Y. Lin, J.-Y. Kuo, M.-K. Wang, and C.-C. Liu, "Removal of methylene blue from aqueous solution using sediment obtained from a canal in an industrial park," *Water Science and Technology*, vol. 78, no. 3, pp. 556–570, 2018.

[2] X. Kang and Z. Chen, "A study of kinetics and thermodynamics of methylene blue adsorption onto the Yellow River bottom sediment," *Materialwissenschaft Und Werkstofftechnik*, vol. 49, no. 11, pp. 392–1398, 2018.

[3] K. Tanji, J. A. Navio, J. Naja et al., "Extraordinary visible photocatalytic activity of a Co0.2Zn0.8O system studied in the Remazol BB oxidation," *Journal of Photochemistry and Photobiology A: Chemistry*, vol. 382, p. 111877, 2019.

[4] K. Tanji, J. A. Navio, A. N. Martín-Gómez et al., "Role of Fe(III) in aqueous solution or deposited on ZnO surface in the photoassisted degradation of rhodamine B and caffeine," *Chemosphere*, vol. 241, p. 125009, 2020.

[5] S. Lairini, "The adsorption of Crystal violet from aqueous solution by using potato peels (*Solanum tuberosum*): equilibrium and kinetic studies," *Journal of Materials and Environmental Science*, vol. 8, no. 9, pp. 3252–3261, 2017.

[6] Y.-L. Ma, Z.-R. Xu, T. Guo, and P. You, "Adsorption of methylene blue on Cu(II)-exchanged montmorillonite," *Journal of Colloid and Interface Science*, vol. 280, no. 2, pp. 283–288, 2004.

[7] H. Shariatmadari, A. R. Mermut, and M. B. Benke, "Sorption of selected cationic and neutral organic molecules on palygorskite and sepiolite," *Clays and Clay Minerals*, vol. 47, no. 1, pp. 44–53, 1999.

[8] K.-T. Chung and S. E. Stevens, "Degradation of azo dyes by environmental microorganisms and helminths," *Environmental Toxicology and Chemistry*, vol. 12, no. 11, p. 2121, 1993.

[9] R. Saravanan, E. Sacari, F. Gracia, M. M. Khan, E. Mosquera, and V. K. Gupta, "Conducting PANI stimulated ZnO system for visible light photocatalytic degradation of coloured dyes," *Journal of Molecular Liquids*, vol. 221, pp. 1029–1033, 2016.

[10] A. Koprdová, M. Bachratá, V. Adamcová, M. Valica, M. Pipíška, and M. Horník, "Chemometric characterization of synthetic dye sorption onto slovakian river sediments: A laboratory batch experiment," *Separations*, vol. 5, 2018.

[11] A. Ksakas, K. Tanji, B. El Bali, M. Taleb, and A. Kherbeche, "Removal of Cu (II) ions from aqueous solution by adsorption using natural clays: kinetic and thermodynamic studies," *Journal of Materials and Environmental Science*, vol. 9, no. 3, pp. 1075–1085, 2018.

[12] J. P. Hu, Y. Liu, H. M. Bi, F. Y. You, and P. T. Xie, "Adsorption of methylene blue from aqueous solution by AB-8 macroreticular resin," *MATEC Web of Conferences*, vol. 60, pp. 8–11, 2016.

[13] Q. Sun and L. Yang, "The adsorption of basic dyes from aqueous solution on modified peat-resin particle," *Water Research*, vol. 37, no. 7, pp. 1535–1544, 2003.

[14] A. Dra, A. El Gaidoumi, K. Tanji, A. Chaouni Benabdallah, A. Taleb, and A. Kherbeche, "Characterization and quantification of heavy metals in Oued Sebou sediments," *The Scientific World Journal*, vol. 2019, Article ID 7496576, 9 pages, 2019.

[15] M. Amar, M. Benzerzour, A. E. M. Safhi, and N.-E. Abriak, "Durability of a cementitious matrix based on treated sediments," *Case Studies in Construction Materials*, vol. 8, pp. 258–276, 2018.

[16] B. Serpaud, R. Al-Shukry, M. Casteignau, and G. Matejka, "Heavy metal adsorption (Cu, Zn, Cd and Pb), by superficial stream sediments: effects of pH, temperature and sediment composition," *Revue Des Sciences De L'Eau*, vol. 7, no. 4, pp. 343–365, 1994.

[17] A. El Gaidoumi, J. M. Doña Rodríguez, E. Pulido Melián et al., "Synthesis of sol-gel pyrophyllite/TiO2 heterostructures: effect of calcination temperature and methanol washing on photocatalytic activity," *Surfaces and Interfaces*, vol. 14, pp. 19–25, 2019.

[18] M. Özacar and İ. A. Şengil, "Adsorption of acid dyes from aqueous solutions by calcined alunite and granular activated carbon," *Adsorption*, vol. 8, no. 4, pp. 301–308, 2002.

[19] J. Gülen, B. Akın, and M. Özgur, "Ultrasonic-assisted adsorption of methylene blue on sumac leaves," *Desalination and Water Treatment*, vol. 57, no. 20, pp. 9286–9295, 2016.

[20] E. O. Oyelude and F. Appiah-Takyi, "Removal of methylene blue from aqueous solution using alkali-modified malted sorghum mash," *Turkish Journal of Engineering and Environmental Sciences*, vol. 36, no. 2, pp. 161–169, 2012.

[21] L. Dali Youcef, L. S. Belaroui, and A. López-Galindo, "Adsorption of a cationic methylene blue dye on an Algerian palygorskite," *Applied Clay Science*, vol. 179, p. 105145, 2019.

[22] A. Günay, E. Arslankaya, and İ. Tosun, "Lead removal from aqueous solution by natural and pretreated clinoptilolite: adsorption equilibrium and kinetics," *Journal of Hazardous Materials*, vol. 146, no. 1-2, pp. 362–371, 2007.

[23] A. J. Lecloux, "Texture of catalysts," in *Catalysis Science & Technology*, J. R. Anderson and M. Boudart, Eds., vol. 2pp. 171–230, 1981.

[24] F. Perche, "Adsorption de polycarboxylates et de lignosulfonates sur poudre modèle et ciments," *école polytechnique fédérale de lausanne*, 2004.

[25] A. Z. Aroguz, J. Gulen, and R. H. Evers, "Adsorption of methylene blue from aqueous solution on pyrolyzed petrified sediment," *Bioresource Technology*, vol. 99, no. 6, pp. 1503–1508, 2008.

[26] J. Gülen and F. Zorbay, "Methylene blue adsorption on a low cost adsorbent-carbonized peanut shell," *Water Environment Research*, vol. 89, no. 9, pp. 805–816, 2017.

[27] R. Calvet, "Le sol-Propriétés et fonctions-Volume 1 Constitution et structure, phénomènes aux interfaces," *Collection Références Scientifiques*, vol. 1, 2003.

[28] Z. Wang, M. Gao, X. Li, J. Ning, Z. Zhou, and G. Li, "Efficient adsorption of methylene blue from aqueous solution by graphene oxide modified persimmon tannins," *Materials Science and Engineering C*, vol. 108, p. 110196, 2019.

[29] M. Khodaie, N. Ghasemi, B. Moradi, and M. Rahimi, "Removal of methylene blue from wastewater by adsorption onto znclactivated corn husk carbon equilibrium studies," *Journal of Chemistry*, vol. 2013, Article ID 383985, 6 pages, 2013.

[30] S. I. Siddiqui, G. Rathi, and S. A. Chaudhry, "Acid washed black cumin seed powder preparation for adsorption of methylene blue dye from aqueous solution: thermodynamic, kinetic and isotherm studies," *Journal of Molecular Liquids*, vol. 264, pp. 275–284, 2018.

[31] G. K. Sarma, S. SenGupta, and K. G. Bhattacharyya, "Methylene blue adsorption on natural and modified clays," *Separation Science and Technology*, vol. 46, no. 10, pp. 1602–1614, 2011.

[32] G. Chcn, J. Pan, B. Han, and H. Yan, "Adsorption of methylene blue on montmorillonite," *Journal of Dispersion Science and Technology*, vol. 20, pp. 1179–1187, 1999.

[33] J. Gülen and M. İ. lenvai, "Removal of methylene blue by using porous carbon adsorbent prepared from carbonized chestnut shell," *Materials Testing*, vol. 59, no. 2, pp. 188–194, 2017.

[34] Z. Bencheqroun, Z. Chaouki, M. Hadri et al., "Removal of textile dyes from aqueous solutions using low cost Moroccan clay," *IOP Conference Series: Earth and Environmental Science*, vol. 161, 2018.

[35] A. A. Basaleh, M. H. Al-Malack, and T. A. Saleh, "Methylene Blue removal using polyamide-vermiculite nanocomposites: kinetics, equilibrium and thermodynamic study," *Journal of Environmental Chemical Engineering*, vol. 7, 2019.

[36] C. A. P. Almeida, N. A. Debacher, A. J. Downs, L. Cottet, and C. A. D. Mello, "Removal of methylene blue from colored effluents by adsorption on montmorillonite clay," *Journal of Colloid and Interface Science*, vol. 332, no. 1, pp. 46–53, 2009.

[37] F. Sakr, S. Alahiane, A. Sennaoui, M. Dinne, I. Bakas, and A. Assabbane, "Removal of cationic dye (methylene blue) from aqueous solution by adsorption on two type of biomaterial of South Morocco," *Materials Today: Proceedings*, vol. 22, pp. 8–11, 2019.